

Synth²: Boosting Visual-Language Models with Synthetic Captions and Image Embeddings

Sahand Sharifzadeh^{*,1}, Christos Kaplani¹, Shreya Pathak¹, Dharshan Kumaran¹, Anastasija Ilic¹, Jovana Mitrovic¹, Charles Blundell¹ and Andrea Banino^{*,1}

^{*}Equal contributions, ¹Google DeepMind

The creation of high-quality human-labeled image-caption datasets presents a significant bottleneck in the development of Visual-Language Models (VLMs). In this work, we investigate an approach that leverages the strengths of Large Language Models (LLMs) and image generation models to create synthetic image-text pairs for efficient and effective VLM training. Our method employs a pretrained text-to-image model to synthesize image embeddings from captions generated by an LLM. Despite the text-to-image model and VLM initially being trained on the same data, our approach leverages the image generator's ability to create novel compositions, resulting in synthetic image embeddings that expand beyond the limitations of the original dataset. Extensive experiments demonstrate that our VLM, finetuned on synthetic data achieves comparable performance to models trained solely on human-annotated data, while requiring significantly less data. Furthermore, we perform a set of analyses on captions which reveals that semantic diversity and balance are key aspects for better downstream performance. Finally, we show that synthesizing images in the image embedding space is 25% faster than in the pixel space. We believe our work not only addresses a significant challenge in VLM training but also opens up promising avenues for the development of self-improving multi-modal models.

Keywords: synthetic data, visual language models, multimodal self-improvement, open-ended learning

1. Introduction

Visual-language models (VLMs) are quickly emerging as powerful tools for understanding visual and textual information. Their ability to combine these two modalities holds immense promise for applications ranging from image captioning to visual question answering. While VLMs hold significant potential, their performance is often constrained by limited data availability. Recent breakthroughs demonstrate that pre-training VLMs on larger image-text pair datasets leads to significant improvements in downstream tasks (Hu et al., 2022; Li et al., 2022b). However, creating such datasets poses several challenges such as scarcity of paired data, potentially noisy nature of data sourced from the internet (e.g., LAION (Schuhmann et al., 2021)), high curation costs, low diversity and high imbalance in semantics. These factors often lead to laborious filtering and extended training times due to low signal-to-noise ratio, thus increasing overall resource consumption (Figure 1A).

This work tackles these limitations by introducing an efficient approach that leverages pretrained generative text and image models to create synthetic paired data for VLMs (see Figure 1B). Our approach uniquely synthesizes both text and images, overcoming the reliance on real-world data and addressing the challenges of scarcity, cost, and noise.

Additionally, the proposed framework operates at both the pixel and embedding levels (see Figure 1C), enabling us to train the VLM from either real images or synthetic image embeddings. This bypasses the need for pixel-space rendering for both the image generator and the VLM encoder. This paradigm shift significantly reduces memory overhead and resource consumption while maintaining the quality of synthetic training data.

While synthetic data generation has been explored for various computer vision tasks such as image segmentation, optical flow prediction, or image classification (Azizi et al., 2023; Fan et al., 2023; Greff et al., 2022; Li et al., 2023c; Mishra

et al., 2022), its application to both visual and textual modalities within VLM training is a significant advancement. Furthermore, a potential pitfall in studying the impact of synthetic data in training new models lies in the inherent advantage of off-the-shelf image generators. These models, trained on massive image-text datasets, may inadvertently equip VLMs with knowledge already embedded in the image generators' own pre-training data. This overlap could mask the true effectiveness of synthetic images, leading to improvements that might be equally achievable by simply training VLMs on the original image generator dataset.

To isolate the unique contribution of synthetic images, we propose a controlled study. Both the text-to-image generator and the VLM undergo pre-training on the exact same dataset. This alignment ensures that any subsequent improvements observed in the VLM after fine-tuning on synthetic data can be confidently attributed to the novel compositions and representations generated, rather than pre-existing knowledge inherited from the original dataset.

To sum up, our research explores the synergy between VLMs and text-to-image generation models, demonstrating a powerful framework for overcoming data limitations. This paper presents the following key contributions:

- **Fully Synthetic Data Creation:** We introduce the first VLM training process that utilizes a fully synthetic dataset of high-quality text-image embedding pairs. These pairs are generated by pre-trained generative models, circumventing the need for massive amounts of real-world data for either modality.
- **Efficient Embedding Space Generation:** Our method works with images in embedding space, avoiding costly image rendering and dramatically improving efficiency, without comprising performance.
- **Fair Evaluation Through Control:** By pre-training a text-to-image model on the same dataset used for VLM training, instead of using a large, off-the-shelf model, we prevent knowledge transfer from a model trained on vast, external image-text pairs. This fosters

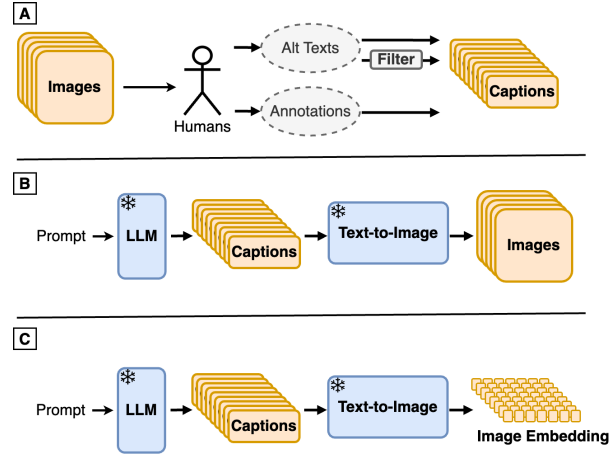


Figure 1 | (A) Traditional dataset curation pipelines require a human in the loop to collect and annotate images. (B) We study whether we can reverse this pipeline with generative models, i.e. by first sampling synthetic captions from an LLM and then synthetically generating images from those. (C) By operating in the image embedding space, we also propose to bypass computationally expensive encoder/decoder steps, optimizing and integrating the process within VLM training.

a fair and focused assessment of the benefits of synthetic data in isolation.

- **Demonstrated Effectiveness:** Experiments will showcase significant performance gains in 3 domains (scene description, scene understanding QA and Extrernal Knowledge QA) when using our synthetic data, assessed against real and synthetic-data baselines.

In conclusion, we offer insights into the future of VLM training, highlighting the potential for creating customized datasets, open-ended training and self-improving multimodal models.

2. Related Work

Visual-language models (VLMs) pretrained on large-scale image-text data, primarily sourced from the web, have shown remarkable capabilities across numerous vision-language tasks. These tasks include image captioning, visual question answering, and few-shot learning (Alayrac et al., 2022; Chen et al., 2022; Li et al., 2022b). Ar-

Table 1 | A taxonomy of related work on synthetic data for training vision models.

Generator	Method	Generator Model	Generated Set	Caption Class	Caption Type	Evaluation Setting
Canonical Concept Mapping	Sharifzadeh et al. (2021) Sharifzadeh et al. (2022)	Linear	Scene Graph Embedding	Scene Graphs Complex Text	Human Generated	SG Classification
Simulation/Rendering Engine	Mishra et al. (2022) Greff et al. (2022) Zheng et al. (2020) de Melo et al. (2022)	Mix	Mixed pairs such as (Segmentation, Images) (Optimal Flow, Videos) (Depth Maps, Images)	N/A	N/A	Mix
	Cascante-Bonilla et al. (2023)		(Captions, Images)		Rule-based	Vision Encoder
Off-the-shelf Image Generator	Azizi et al. (2023) Fan et al. (2023)	SD Imagen MUSE	Images	Single Word	ImageNet Classes	Classifier
	Li et al. (2023c)					
Controlled Image Generator	Synth ²	MUSE	Text, Embeddings & Images	Complex Text	Human & LLM Generated	VLM

chitecturally, VLMs commonly employ an image encoder coupled with a large language model (LLM). Researchers explore diverse image encoder designs, ranging from convolutional neural networks (CNNs) (Alayrac et al., 2022) to transformer-based architectures (Chen et al., 2022). Additionally, the choice between pre-training the image encoder on separate image datasets (Alayrac et al., 2022) and training it from scratch alongside the VLM (Tsimpoukelli et al., 2021) remains an active area of investigation. Pretraining VLMs involves various objectives, including supervised learning approaches, as well as contrastive methods that focus either on aligning image and text representations (Radford et al., 2021) or on aligning different image representations (Chen et al., 2020a,b; Grill et al., 2020). Similar diversity exists in LLM choices, with both encoder-decoder (Chen et al., 2022) and decoder-only (Alayrac et al., 2022) architectures being utilized. The strategies for combining information extracted by the image encoder and the language model also exhibit substantial variation. Despite the success achieved with web-scraped datasets, there's a growing emphasis on designing VLM architectures that facilitate training using synthetically generated data. This capability holds particular significance for applications where data scarcity or resources availability pose significant challenges.

Generation of synthetic data for training machine learning models remains a highly active area of research. While numerous studies (Cascante-Bonilla et al., 2023; de Melo et al., 2022; Greff et al., 2022; Mishra et al., 2022; Zheng et al., 2020) explore the use of model-based rendering engines or simulators, the remarkable advancements in high-quality image

generators have ignited a surge of interest in leveraging generative models for creating training data. This trend has significantly impacted a wide range of computer vision tasks, including semantic segmentation (Baranchuk et al., 2021; Chen et al., 2019; Li et al., 2021, 2022a; Ros et al., 2016; Tritrong et al., 2021), human motion understanding (Guo et al., 2022; Ma et al., 2022; Varol et al., 2017), and more recently image classification (Azizi et al., 2023; Fan et al., 2023). Our work investigates the potential of data-driven generative models within the domain of visual-language models (VLMs). We focus on their application in downstream tasks, where the ability to process complex scene is important. From this aspect, our approach is closest to a concurrent work by Li et al. (2023c) where the goal is to replace faulty images in a captioning pipeline with their synthetic versions. However, our work distinguishes itself from Li et al. (2023c) by achieving strong performance while utilizing 40 times less paired data and only a quarter of the parameters. This demonstrates the potential for achieving both performance and efficiency through our proposed approach. Furthermore, unlike the mentioned works (Azizi et al., 2023; Fan et al., 2023; Li et al., 2023c), we avoid using an off-the-self image generator trained on larger datasets. This approach prevented knowledge transfer into the VLM from a model trained on large amounts of paired data, which is critical as such knowledge transfer would have obscured our ability to scientifically assess the unique contribution of synthetic data.

Our work can also be likened to the concept of cycle consistency (Zhu et al., 2017) in visual-language models. This principle, where image-to-text and text-to-image conversion can be em-

ployed as a form of synthetic data training, albeit with extra gradients throughout the network, exploring image-text cycle consistency during sampling (Li et al., 2023a) or training (Li et al., 2023b) has been explored in recent works, demonstrating promising results.

Finally, we emphasize the efficiency of pipelines that seamlessly connect data generation and model training. While most prior work has concentrated on generating images in pixel space, we investigate the generation of image embeddings that can be directly integrated into the VLM. Our approach aligns with recent work in the scene graph classification domain (Sharifzadeh et al., 2021, 2022), which has explored synthetic scene graph embedding generation using pretrained canonical class representations.

Table 1 provides a taxonomy of some of the mentioned related work to clarify the differences better. As shown, our study is the first of its kind to scientifically explore the application of synthetic data generation within a VLM training pipeline and in particular using image embeddings and by generating synthetic captions.

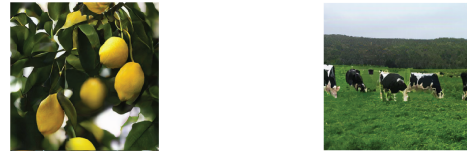
3. Synth²

Given the synthetic generation of text and then images, we refer to our method as Synth². Synth² is a pipeline for training VLMs using generative models in addition to collected human data. In this section we introduce different components of this pipeline, namely Caption Generation, Image Generation and the full Synth² model (see Figure 3 for details).

3.1. Synthetic Caption Generation

We leverage the generative capabilities of LLMs to create synthetic captions. To ensure a wide variety of captions, we adopt a class-based prompting approach. First, we randomly select a class from the ImageNet21k dataset (Ridnik et al., 2021). The LLM (Gemini Pro (Team et al., 2023)) is then prompted with the following text:

Make up a human-annotated description of an image that contains the following object: [object].



This is an image of a lemonwood tree with dark green leaves and straight, slim branches with bright yellow lemons hanging from them.



This is an image of a field of dairy cattle grazing on grass, with some trees in the background.



This is an image of a small white bowl filled with a light yellow, creamy substance known as aioli, set against a neutral-colored background.



This is an image of a sports team during a game, where the players wear matching uniforms and run forward on a grassy field.

Figure 2 | Examples of synthetic captions and synthetic images generated by LLM and text-to-image generator.

The caption should be around 30-40 words long. Describe the different components of the scene in an objective and unbiased way. Do not add subjective judgments about the image, it should be as factual as possible. Do not use fluffy, poetic language. Respond only with the caption itself, beginning with “This is an image of”.

where we replace “[object]” with the randomly selected class. This class-based prompting encourages the LLM to generate captions that cover a broad range of visual concepts. Figure 2 shows some samples from the generated captions.

3.2. Image Generation

Our image generator architecture is similar to Chang et al. (2023) and was chosen for its superior inference efficiency due to parallel decoding and its use of discrete image tokens that dramatically reduces the number of sampling iterations compared to auto-regressive models. Additionally, MUSE leverages a transformer architecture, further enhancing efficiency (Chang et al., 2023). As discussed in Section 1, to mitigate the potential for knowledge overlap between off-the-shelf image generators and VLMs, we deviate from standard practice. Instead of employing pre-trained image generators, we intentionally pre-train both our text-to-image generator and VLM

on an identical dataset. This controlled setup ensures that any performance gains observed in the VLM after fine-tuning on the synthetic data are directly attributable to the unique contributions of the generated images, rather than inherited knowledge from the original dataset. Hence, we pretrain an image generator on a image-caption dataset that will also be utilized for VLM pretraining (i.e. Conceptual Captions v2 (Changpinyo et al., 2021) see Section 4).

3.2.1. Training

To pretrain our image generator given paired image and texts, we embed the texts with a pre-trained language model and the images with a pre-trained VQ-GAN (Esser et al., 2021) (refer to A.1.1 in the appendix for the details). The pre-trained language model is the same used in our VLM and it is a reduced version of Chin-chilla (Hoffmann et al., 2022) using 400 million parameters. Following the approach in Chang et al. (2023), we apply a masking procedure with a cosine scheduling function. This function gradually increases the masking ratio during training, biasing the model towards learning from images with larger masked regions. On average, around 64% of the VQ tokens are replaced with a special “dropped token”. The noisy VQ tokens and the embedded text are then fed into a transformer model. The model’s objective is to predict the original, unmasked VQ tokens. The loss function is the cross-entropy between the predicted VQ tokens and the masked ones:

$$L_{t2i} = \prod_{t \in M} p(z(x)_t | y, \{z(x)_u | u \notin M\}),$$

where $z(x)$ denotes the VQ tokens computed from the ground-truth image x , y denotes the ground-truth caption, and M denotes the indices of the masked tokens. Our text-to-image generator was trained only on 10.1 millions text-image pairs from Conceptual Captions V2 (Changpinyo et al., 2021) (see Section 4 for details).

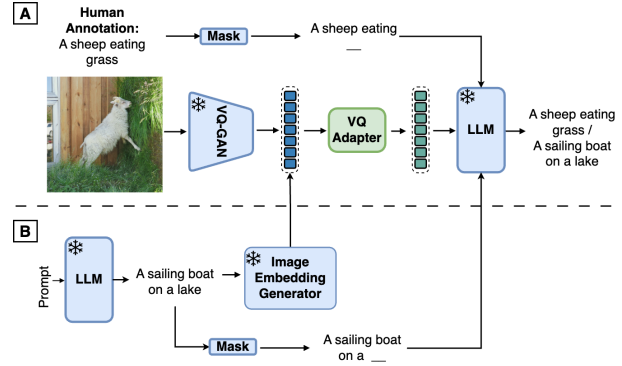


Figure 3 | We introduce a VLM framework that leverages LLMs and image generation models to create synthetic image-text pairs for efficient training. We can train a VLM from both non-synthetic (A) and synthetic (B) data as shown in this figure. Our model trained with the added synthetic pairs demonstrates impressive image captioning performance, significantly reducing the need for human annotated images.

3.2.2. Inference

During inference, we use an iterative procedure to generate images. At first iteration, the predicted VQ tokens are all initialized with the “dropped token” representing the masked entries. At each upcoming iteration, the text embedding and the predicted VQ tokens until that stage are fed into the transformer and the model predicts the masked tokens. A cosine schedule determines which masked tokens have the highest prediction confidence during decoding. These tokens are unmasked, progressively reducing the masked token set. This process repeats for 24 iterations, gradually refining the generated VQ-tokens. Additional details for our text-to-image generator model and examples of generated images, given ground truth annotations compared to the original ones, are reported in A.1.3 in the appendix.

3.3. Synth² VLM architecture

As described in Section 3.2, our text-to-image model generates image embeddings through an iterative caption-conditioned denoising process. A VQ-GAN decoder could be used to convert these tokens into human-viewable images. However, we emphasize that the image embeddings them-

selves provide a compressed representation of an image, making the decoder step unnecessary for certain applications.

Therefore, to enhance efficiency for training the VLM from synthetic data, we design the VLM to enable the bypass of pixel-space processing. This is achieved by setting its vision encoder to be identical to the VQ-GAN backbone used for our image generator. This enables seamless interaction between the VLM and synthetically generated image embeddings and eliminates the computationally expensive decoding stage of VQ-GAN for the image generator and the encoding stage for the VLM when training on synthetic data. At the same time, it still allows us to train from images in pixel space when using human annotated data. This design feature is particularly important since in order to curtail model collapse effects (Shumailov et al., 2023), we need to mix synthetic and real data during finetuning (Gerstgrasser et al., 2024).

Overall, our VQ-based design removes the need for costly conversions to and from pixel space, resulting in significant time and disk space savings as will be shown in Section 4. To harness the efficiency of discrete tokens during training and sampling, while maintaining the rich image understanding provided by soft embeddings, we convert each discrete token to its soft embedding using the codebook before feeding them to the VLM.

On top of the VQ backbone in our VLM, we incorporate a Perceiver Resampler component (Jaegle et al., 2021) to cross-attend to the VQ tokens extracted from our backbone. Similar to Flamingo Alayrac et al. (2022), we employ a frozen language model to cross-attend to the image representation and autoregressively generate text. While the self-attention layers in the language model remain frozen, the cross-attention layers between the language and vision components are trainable, allowing the model to learn effective multimodal representations.

The VLM’s objective is to predict the next token in a sequence, conditioned on the input image. This is formulated as a cross-entropy loss:

$$L_{VLM} = \prod_{l=1}^L p(y_l|y_{<l}, x), \quad (1)$$

where x denotes the image, y_l represents the l -th language token, and $y_{<l}$ represents all tokens preceding y_l . As shown in Figure 3 by combining the components introduced in the previous parts, we can train VLMs either from human annotated data or synthetic image-captions pairs such that the VLM is conditioned on the synthetic image embedding with the cross-entropy loss being between the synthetic captions and the VLM’s predictions.

4. Experiments

4.1. Experimental setup

4.1.1. Datasets

For training we used four datasets: (1) **Conceptual Captions v2** (Changpinyo et al., 2021) (CCv2) is a dataset with 12 million image-text pairs that are collected by automatically extracting images and their corresponding “alt-tex” descriptions from various websites. In our experiments we use CCv2 as the main source of human-annotated data whereas for the other datasets we might use synthetically generated images/texts depending on the experiment. (2) **WebLI** (Chen et al., 2022) has around 350 million image and alt text pairs with high text quality in English. (3) **LTIP** (Alayrac et al., 2022) has 312 million web collected image and text pairs. (4) **GenPair** refers to 1 million fully synthetic captions paired with synthetic images generated that we create on-the-fly during the VLM training using our text-to-image generator. The details are described in Section 3.1.

We tested our model on 3 different domains:

- **Scene description:** for this task we used MS-COCO (Chen et al., 2015) and we evaluate the performance of our models on the commonly used test set of MS-COCO under zero-shot and fine-tuning settings. For the finetuning settings we use the training set

MS-COCO. We use the Karpathy split (Karpathy and Fei-Fei, 2015) for evaluation. Another dataset we used for this class is Flickr-30k (Plummer et al., 2015): again, we evaluate performances on the Karpathy split. We use CIDEr score (Vedantam et al., 2015) as our metric.

- **Scene understanding QA:** for this task we used VQAv2 (Goyal et al., 2017) and we evaluated on the test-dev set. We use VQA accuracy (Antol et al., 2015) as our metric.
- **External knowledge QA:** for this task we used OKVQA (Marino et al., 2019) and we evaluated on the validations set as in Alayrac et al. (2022). We use VQA accuracy (Antol et al., 2015) as our metric.

4.1.2. Training details

For both the image generator and the VLM we use a pre-trained and frozen VQ-GAN (see A.1.1 for details on the network). The images are input at a resolution of 256x256, with a patch size of 16, which results in a sequence length of 256 tokens (16x16). Both models use a pre-trained and frozen Chinchilla 400m (Hoffmann et al., 2022) as LLM. The VLM has a perceiver resampler (Alayrac et al., 2022; Jaegle et al., 2021) with 6 layers and 64 latent input queries that cross-attend to the image embeddings. There are cross attention layers between each layer in the LLM and the output of perceiver resampler similar to (Alayrac et al., 2022) (refer to A.1.4 for details).

We use ViT-B (Dosovitskiy et al., 2020) for the main text-to-image model in the image generator (see Appendix A.1.3 for full details), with a maximum text length of 64 tokens with guidance scale of 4.0, 24 refining steps and a sample choice temperature of 32.5. All the models are trained with AdamW (Loshchilov and Hutter, 2017) with a learning rate of 0.0001, 5000 warmup steps, and the batch size of 512. For fine-tuning settings (on COCO), we use a learning rate of 0.00001. Section A.1.3 reports additional details. We pre-train the image generator for 500k steps at which point it has a Fréchet inception distance (FID) (Heusel et al., 2017) of 17.1 on MS-COCO test pairs. Our VLMs training experi-

ments all run for 500k steps. Our models are all implemented in JAX and trained on 256 TPUs.

4.2. Results

4.2.1. Synthetic Images

To first assess the effectiveness of synthetic images compared to the original ones in VLM training, we conduct a study where human-written captions from existing datasets are paired with synthetic images generated by a text-to-image model. We train a VLM on these synthetic image-caption pairs and evaluate its performance against a model trained on the original real image-caption pairs. This comparison allows us to investigate whether synthetic images can effectively substitute for real images in the context of VLM training.

Specifically, we generate synthetic images for the LTIP and WebLI datasets using their annotations. This provides us with (*Real Text, Synthetic Image*) pairs to train a VLM with (Synth² in Table 2). We compare this model to the model trained on the human-annotated data of Conceptual Caption v2 (CCv2) only, using no data from LTIP and WebLI (**Baseline**) and the models trained on the original (*Real Text, Real Image*) pairs (**Gold** in Table 2). For consistency, and to reduce model collapse, all Synth² and Gold models are co-trained with CCv2, the same dataset used by our text-to-image generator and the baseline.

As shown in Table 2, synthetic images significantly improve baseline model performance across the full set of downstream tasks. Importantly, they are effective for VLM training despite the smaller volume of human-annotated images used. Note that “Gold” represents the upper performance bound when using the full original dataset. For LTIP, synthetic images slightly outperform original images, likely due to increased data diversity; while original pairs remain static during training, synthetic images introduce beneficial image augmentation (Azizi et al., 2023).

These results suggest the potential of generative models to enhance VLM training containing complex, multi-object scenes and detailed captions, even with limited real image data.

Table 2 | Zero shot image captioning results when training with ground truth captions paired with either the original or synthetically generated images.

Method	Real	Synth	#Real Data	#Synth Data	CIDEr-COCO (\uparrow)	CIDEr-Flickr-30 (\uparrow)	VQAV2 Accuracy (\uparrow)	OKVQA Accuracy (\uparrow)
Baseline	CCv2	-	10.1M	-	22.1	12.7	29.1	32.4
Synth ²	CCv2	LTIP	10.1M	330M	28.7	16.7	33.5	34.5
	CCv2	WebLI	10.1M	350M	27.6	18.1	34.1	34.7
	CCv2	WebLI+LTIP	10.1M	670M	33.4	20.8	35.3	36.1
Gold	CCv2+LTIP	-	340.1M	-	27.6	20.9	36.7	38.1
	CCv2+WebLI	-	360.1M	-	30.7	21.1	36.2	38.5
	CCv2+LTIP+WebLI	-	690.1M	-	35.3	23.4	37.9	39.4

Table 3 | Zero shot results when using synthetically generated caption and image embedding pairs. Concentration is calculated as the cumulative distribution on the top-5 clusters, a lower value represent higher diversity (see Appendix A.3 for more details).

Real	Synth	#Real Data	#Synth Data	Concentration (\downarrow)	Entropy (\uparrow)	CIDEr-COCO (\uparrow)	Flickr-30(\uparrow)	VQAV2 Acc. (\uparrow)	OKVQA Acc. (\uparrow)
CCv2	-	10.1M	-	-	-	22.1	12.7	29.1	32.4
CCv2	GenPair	10.1M	1M	57.7%	3.81	25.9	17.3	31.1	34.0
CCv2+WebLI	-	10.1M+1M	-	69.8%	3.43	24.4	14.9	30.6	33.9
CCv2+LTIP	-	10.1M+1M	-	83.0%	2.92	23.4	13.8	30.3	32.9

4.2.2. Synthetic text and image pairs

To further demonstrate the efficacy of using synthetic data for VLM training, we conducted additional experiments where the entire dataset including captions and their corresponding images are generated synthetically by an LLM and the image generator (see Section 2 for the explanation of how these caption where generate and Figure 1D for some examples).

Comparing the first two rows in Table 3 shows that adding even a small fraction (1M) of purely synthetic image-caption data (GenPair) significantly improves performance across all evaluated domains. Interestingly, sampling an additional 1M data points from *real* datasets like WebLI or LTIP (rows 3 and 4) yields lower improvement.

To investigate this, we assessed the semantic diversity and balance of each caption set. First, we used our language model to generate embeddings for the synthetic GenPair and the real WebLI and LTIP captions. Then, we employed k-means clustering to analyze these embeddings (see Appendix A.3 for details). Figure 4 shows the cluster distribution among all three datasets, with the x-axis representing the cluster index and the y-axis representing data volume from each dataset within a cluster. Notice how LTIP and WebLI have

a large concentration of data only within clusters 19, 18, 1, 16 and 0, while most other clusters are under-populated. In contrast, GenPair is distributed more evenly across different clusters (e.g. clusters 1, 4, 6, 9, 12, 14, 15, 16, 17, 18 are all well populated), suggesting superior balance compared to the other two.

To quantify the mentioned semantic concentration within each dataset we use a “Concentration Metric” as the percentage of data belonging to the top-5 most populated clusters. As reported in Table 3, GenPair has the lowest concentration, with only 57.5% of its captions in the top-5 clusters. This indicates lower semantic imbalance in the synthetically generated GenPair and contrasts with the higher imbalance found in the other datasets (69.9% and 83%). Also, the entropy over the full cluster distribution, confirms that GenPair has a more uniform distribution of data across clusters. We postulate that the inherent diversity within GenPair likely contributes to its robust performance on downstream tasks, as models trained on diverse data tend to generalize better.

This evaluation demonstrates Synth²’s capacity to leverage diverse text data, including synthetic data, for enhanced performance. Our proposed analysis and metrics can inform synthetic data

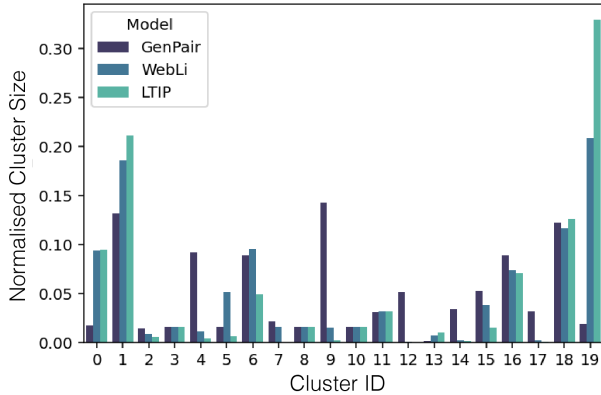


Figure 4 | Semantic diversity. Histogram represent the distribution of cluster sizes, with GenPair showing a more uniform coverage of semantic concepts. See A.3 for details on how the histogram was derived.

creation, further optimizing its impact. Notably, our findings highlight the significant role of synthetic data, generated via image synthesis and LLM captions, in overcoming data limitations and boosting VLM capabilities. This underscores the effectiveness of text-only captions for model enhancement, emphasizing the value of our technique.

4.2.3. Comparison with related work

Furthermore, we investigated the potential of our approach compared to the state-of-the-art model while taking into account the amount of synthetic or real training data and the number of model parameters. We combined all the three datasets namely, GenPair, WebLI and LTIP. Table 4 compares our model’s MS-COCO benchmark performance against related methods: ITIT (Li et al., 2023b), DC (Li et al., 2023c) and SimVLM (Wang et al., 2021). Note that, in this case we provide both zero-shot and finetuning results (see Section A.2 in the Appendix). ITIT employs cycle consistency for VLM improvement, while DC uses Stable Diffusion to generate images based on human-defined heuristics, and SimVLM has one of the state-of-the-art performances on MS-COCO.

Synth² and ITIT share similar parameter counts and paired data usage, making them directly comparable. As shown in Table 4, Synth² drastically outperforms ITIT on the CIDEr score. While

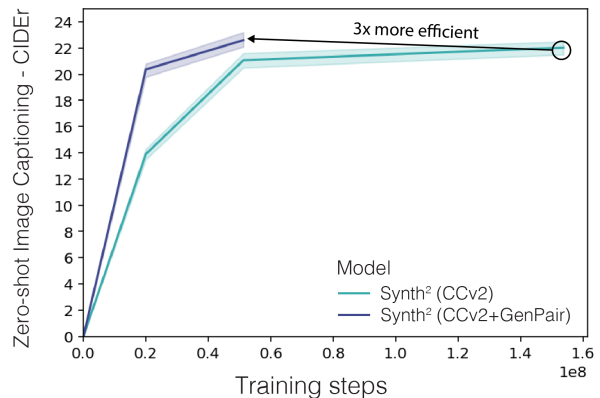


Figure 5 | Performance as a function of training steps. The blue curve shows the baseline trained solely on paired data (CCv2). The purple curve demonstrates Synth²’s performance trained additionally on augmentation with fully synthetic data (GenPair). Synth² achieves parity with the baseline using roughly 1/3 of the training steps, showcasing its superior efficiency. Shaded regions represent standard deviation across 3 random seeds.

DC achieves the highest raw performance, it requires significantly more parameters, relies on vast amount of real data, and the filtering procedure is heavily based on human heuristics.

Synth² strikes a balance between performance and efficiency. By leveraging text-only data, it achieves competitive results using 40 times less paired data than DC. Interestingly, despite performing weaker than SimVLM on finetuning, Synth² has the highest in zero-shot performance among all models. This comparison highlights the trade-offs between performance, efficiency, and data requirements. Synth² emerges as a compelling solution when resources are limited, achieving impressive results with reduced data and computational overhead.

4.2.4. Extra analysis

To further analyze the boost in performance afforded by augmentation with fully synthetic data, we characterized the performance of the baseline model (i.e. trained solely on CCv2), and Synth² which was additionally trained together with GenPair. Figure 5 visualizes the perfor-

Table 4 | Zero shot and fine tuning results, comparison with related work. The image-captioning performance is evaluated on the COCO Karpathy split. Bold indicates the best and underline the second best values.

Model	#All Params↓	#Real Data↓	#Synth Data↓	CIDEr↑ (FT)	CIDEr↑ (zs)
ITIT	11.2B	3M	110M	103.5	32.1
DC (BLIP)	1.7B	5.5B	400M	<u>133.1</u>	-
SimVLM	1.4B	1.1B	365M	143.3	32.2
Synth ²	632M	10.1M	711M	131.3	35.4

mance trends for both models. Notably, the light blue curve representing the baseline exhibits a gradual increase in performance with increasing training steps, eventually plateauing at 22.1 CIDEr score. In contrast, the purple curve reveals Synth²'s steeper performance improvement, achieving comparable performance to the paired only training regime, with roughly 1/3 of the training steps. This highlights the significant data efficiency gain achieved through fully synthetic data augmentation in Synth². Shaded regions surrounding each curve indicate standard deviation across three random seeds, demonstrating the robustness of the observed performance trends. These findings demonstrate Synth²'s ability to effectively leverage fully synthetic data, resulting in remarkable performance gains.

Our study also investigated the computational efficiency of Synth². We compared the case where captions are used to generate image embedding versus when captions are rendered into actual images. As shown in Table 5, Synth² trained using image embedding consistently demonstrates faster performance, running at 2.08 training steps per second, whereas Synth² trained from pixel runs at a slower pace of 1.66 steps/second. Critically, the performance on image captioning and visual question answering are not affected. This efficiency advantage stems from Synth²'s utilization of text-only data and embedding-based image generation using parallel decoding, which reduces the computational overhead associated with processing pixel-based images as done in the Synth² model trained from pixels without affecting the performance. For further studies, e.g. comparing the performance of different image encoder backbones refer to Appendix, Table 9.

Table 5 | Model efficiency measured by computing the steps per second of training on the same hardware. Synth² in embedding space consistently outperforms the Synth² using pixels, demonstrating superior training efficiency.

Model	Step/Sec↑	MSCOCO CIDEr(zs)↑	VAQV2 Accuracy (ft)↑
Synth ² - Embeddings	2.08	25.9	50.1
Synth ² - Pixels	1.66	26.0	49.9

5. Limitations

The two main limitations of the current work stem from the restricted quantity of fully synthetic data used and the limited exploration of text data sources. Firstly, whilst we were able to show a substantial gain when training was augmented with fully synthetic data, our experiments were limited to a relatively low quantity of data (i.e. 1M image-caption pairs). In the future, it will be important to examine whether using orders of magnitude more fully synthetic data (e.g. ~700M) will result in performance gains that surpass that of using solely paired data. Also, the current work primarily explores a restricted set of text-only data sources. Further research is necessary to investigate the potential of diverse text sources, including investigating context-specific generation (e.g., medical data), which could be an exciting avenue for future exploration. By acknowledging and addressing these limitations, future research can leverage the strengths of the Synth² approach and enhance its generalizability, robustness, and efficiency for a broader range of visual-language modeling tasks.

6. Conclusions

Our study presents a novel approach for generating synthetic image-text pairs to enhance the training of visual language models. By harnessing the capabilities of large language models and text-to-image generation, we effectively address the limitations of manual image labeling such as scalability, customization and costs. In particular, we show that the visual language model trained on our synthetic and human annotated datasets exhibits a marked improvement in image captioning tasks compared to a baseline trained

exclusively on human-annotated data. Overall, this research introduces a novel technique that has the potential to transform visual language model training. Our findings highlight the value of synthetic data generation, paving the way for advancements in numerous fields where visual language understanding is crucial.

7. Broader Impact

This paper presents work whose goal is to advance the field of Machine Learning. There are many potential societal consequences of our work, none which we feel must be specifically highlighted here. In particular biases in generative models can have a drastic effect on the synthetic data. Similarly it is important to consider the challenges of privacy when using generative models.

Acknowledgements

We would like to thank Sander Dieleman, Ali Razavi, and Benigno Uria for their insights on VQGAN. We would also like to thank Aida Nematzadeh, Pinelopi Papalampidi, Han Zhang, Mateusz Malinowski, Valentin De Bortoli, Sahra Ghalebikesabi, Emanuele Bugliarello, Chris Knutson, and Murray Shanahan for their in depth comments and support throughout the project.

References

J.-B. Alayrac, J. Donahue, P. Luc, A. Miech, I. Barr, Y. Hasson, K. Lenc, A. Mensch, K. Millican, M. Reynolds, et al. Flamingo: a visual language model for few-shot learning. *Advances in Neural Information Processing Systems*, 35: 23716–23736, 2022.

S. Antol, A. Agrawal, J. Lu, M. Mitchell, D. Batra, C. L. Zitnick, and D. Parikh. Vqa: Visual question answering. In *Proceedings of the IEEE international conference on computer vision*, pages 2425–2433, 2015.

S. Azizi, S. Kornblith, C. Saharia, M. Norouzi, and D. J. Fleet. Synthetic data from diffusion models improves imagenet classification. *arXiv preprint arXiv:2304.08466*, 2023.

D. Baranchuk, I. Rubachev, A. Voynov, V. Khrulkov, and A. Babenko. Label-efficient semantic segmentation with diffusion models. *arXiv preprint arXiv:2112.03126*, 2021.

A. Brock, S. De, S. L. Smith, and K. Simonyan. High-performance large-scale image recognition without normalization. In *International Conference on Machine Learning*, pages 1059–1071. PMLR, 2021.

P. Cascante-Bonilla, K. Shehada, J. S. Smith, S. Doveh, D. Kim, R. Panda, G. Varol, A. Oliva, V. Ordonez, R. Feris, et al. Going beyond nouns with vision & language models using synthetic data. In *Proceedings of the IEEE/CVF International Conference on Computer Vision*, pages 20155–20165, 2023.

H. Chang, H. Zhang, J. Barber, A. Maschinot, J. Lezama, L. Jiang, M.-H. Yang, K. Murphy, W. T. Freeman, M. Rubinstein, et al. Muse: Text-to-image generation via masked generative transformers. *arXiv preprint arXiv:2301.00704*, 2023.

S. Changpinyo, P. Sharma, N. Ding, and R. Soricut. Conceptual 12m: Pushing web-scale image-text pre-training to recognize long-tail visual concepts. In *Proceedings of the IEEE/CVF Conference on Computer Vision and Pattern Recognition*, pages 3558–3568, 2021.

T. Chen, S. Kornblith, M. Norouzi, and G. Hinton. A simple framework for contrastive learning of visual representations. In *International conference on machine learning*, pages 1597–1607. PMLR, 2020a.

T. Chen, S. Kornblith, K. Swersky, M. Norouzi, and G. E. Hinton. Big self-supervised models are strong semi-supervised learners. *Advances in neural information processing systems*, 33: 22243–22255, 2020b.

X. Chen, H. Fang, T.-Y. Lin, R. Vedantam, S. Gupta, P. Dollár, and C. L. Zitnick. Microsoft coco captions: Data collection and evaluation server. *arXiv preprint arXiv:1504.00325*, 2015.

X. Chen, X. Wang, S. Changpinyo, A. Piergiovanni, P. Padlewski, D. Salz, S. Goodman, A. Grycner, B. Mustafa, L. Beyer, et al. Pali: A jointly-scaled multilingual language-image model. *arXiv preprint arXiv:2209.06794*, 2022.

Y. Chen, W. Li, X. Chen, and L. V. Gool. Learning semantic segmentation from synthetic data: A geometrically guided input-output adaptation approach. In *Proceedings of the IEEE/CVF conference on computer vision and pattern recognition*, pages 1841–1850, 2019.

C. M. de Melo, A. Torralba, L. Guibas, J. DiCarlo, R. Chellappa, and J. Hodgins. Next-generation deep learning based on simulators and synthetic data. *Trends in cognitive sciences*, 2022.

A. Dosovitskiy, L. Beyer, A. Kolesnikov, D. Weissenborn, X. Zhai, T. Unterthiner, M. Dehghani, M. Minderer, G. Heigold, S. Gelly, et al. An image is worth 16x16 words: Transformers for image recognition at scale. *arXiv preprint arXiv:2010.11929*, 2020.

P. Esser, R. Rombach, and B. Ommer. Taming transformers for high-resolution image synthesis. In *Proceedings of the IEEE/CVF conference on computer vision and pattern recognition*, pages 12873–12883, 2021.

L. Fan, K. Chen, D. Krishnan, D. Katabi, P. Isola, and Y. Tian. Scaling laws of synthetic images for model training... for now. *arXiv preprint arXiv:2312.04567*, 2023.

M. Gerstgrasser, R. Schaeffer, A. Dey, R. Rafailov, H. Sleight, J. Hughes, T. Korbak, R. Agrawal, D. Pai, A. Gromov, et al. Is model collapse inevitable? breaking the curse of recursion by accumulating real and synthetic data. *arXiv preprint arXiv:2404.01413*, 2024.

Y. Goyal, T. Khot, D. Summers-Stay, D. Batra, and D. Parikh. Making the v in vqa matter: Elevating the role of image understanding in visual question answering. In *Proceedings of the IEEE conference on computer vision and pattern recognition*, pages 6904–6913, 2017.

K. Greff, F. Belletti, L. Beyer, C. Doersch, Y. Du, D. Duckworth, D. J. Fleet, D. Gnanapragasam, F. Golemo, C. Herrmann, et al. Kubric: A scalable dataset generator. In *Proceedings of the IEEE/CVF Conference on Computer Vision and Pattern Recognition*, pages 3749–3761, 2022.

J.-B. Grill, F. Strub, F. Altché, C. Tallec, P. Richemond, E. Buchatskaya, C. Doersch, B. Avila Pires, Z. Guo, M. Gheshlaghi Azar, et al. Bootstrap your own latent-a new approach to self-supervised learning. *Advances in neural information processing systems*, 33:21271–21284, 2020.

X. Guo, W. Wu, D. Wang, J. Su, H. Su, W. Gan, J. Huang, and Q. Yang. Learning video representations of human motion from synthetic data. In *Proceedings of the IEEE/CVF Conference on Computer Vision and Pattern Recognition*, pages 20197–20207, 2022.

M. Heusel, H. Ramsauer, T. Unterthiner, B. Nessler, and S. Hochreiter. Gans trained by a two time-scale update rule converge to a local nash equilibrium. *Advances in neural information processing systems*, 30, 2017.

J. Hoffmann, S. Borgeaud, A. Mensch, E. Buchatskaya, T. Cai, E. Rutherford, D. d. L. Casas, L. A. Hendricks, J. Welbl, A. Clark, et al. Training compute-optimal large language models. *arXiv preprint arXiv:2203.15556*, 2022.

X. Hu, Z. Gan, J. Wang, Z. Yang, Z. Liu, Y. Lu, and L. Wang. Scaling up vision-language pre-training for image captioning. In *Proceedings of the IEEE/CVF conference on computer vision and pattern recognition*, pages 17980–17989, 2022.

A. Jaegle, F. Gimeno, A. Brock, O. Vinyals, A. Zisserman, and J. Carreira. Perceiver: General perception with iterative attention. In *International conference on machine learning*, pages 4651–4664. PMLR, 2021.

A. Karpathy and L. Fei-Fei. Deep visual-semantic alignments for generating image descriptions. In *Proceedings of the IEEE conference on computer vision and pattern recognition*, pages 3128–3137, 2015.

D. P. Kingma and J. Ba. Adam: A method for stochastic optimization. *arXiv preprint arXiv:1412.6980*, 2014.

D. Li, J. Yang, K. Kreis, A. Torralba, and S. Fidler. Semantic segmentation with generative models: Semi-supervised learning and strong out-of-domain generalization. In *Proceedings of the IEEE/CVF Conference on Computer Vision and Pattern Recognition*, pages 8300–8311, 2021.

D. Li, H. Ling, S. W. Kim, K. Kreis, S. Fidler, and A. Torralba. Bigdatasetgan: Synthesizing imagenet with pixel-wise annotations. In *Proceedings of the IEEE/CVF Conference on Computer Vision and Pattern Recognition*, pages 21330–21340, 2022a.

H. Li, J. Gu, R. Koner, S. Sharifzadeh, and V. Tresp. Do dall-e and flamingo understand each other? In *Proceedings of the IEEE/CVF International Conference on Computer Vision*, pages 1999–2010, 2023a.

J. Li, D. Li, C. Xiong, and S. Hoi. Blip: Bootstrapping language-image pre-training for unified vision-language understanding and generation. In *International Conference on Machine Learning*, pages 12888–12900. PMLR, 2022b.

T. Li, S. Bhardwaj, Y. Tian, H. Zhang, J. Barber, D. Katabi, G. Lajoie, H. Chang, and D. Krishnan. Leveraging unpaired data for vision-language generative models via cycle consistency. *arXiv preprint arXiv:2310.03734*, 2023b.

W. Li, J. F. Lotz, C. Qiu, and D. Elliott. Data curation for image captioning with text-to-image generative models. *arXiv preprint arXiv:2305.03610*, 2023c.

I. Loshchilov and F. Hutter. Decoupled weight decay regularization. *arXiv preprint arXiv:1711.05101*, 2017.

J. Ma, S. Bai, and C. Zhou. Pretrained diffusion models for unified human motion synthesis. *arXiv preprint arXiv:2212.02837*, 2022.

K. Marino, M. Rastegari, A. Farhadi, and R. Mottaghi. Ok-vqa: A visual question answering benchmark requiring external knowledge. In *Proceedings of the IEEE/cvpr conference on computer vision and pattern recognition*, pages 3195–3204, 2019.

S. Mishra, R. Panda, C. P. Phoo, C.-F. R. Chen, L. Karlinsky, K. Saenko, V. Saligrama, and R. S. Feris. Task2sim: Towards effective pre-training and transfer from synthetic data. In *Proceedings of the IEEE/CVF Conference on Computer Vision and Pattern Recognition*, pages 9194–9204, 2022.

B. A. Plummer, L. Wang, C. M. Cervantes, J. C. Caicedo, J. Hockenmaier, and S. Lazebnik. Flickr30k entities: Collecting region-to-phrase correspondences for richer image-to-sentence models. In *Proceedings of the IEEE international conference on computer vision*, pages 2641–2649, 2015.

A. Radford, J. W. Kim, C. Hallacy, A. Ramesh, G. Goh, S. Agarwal, G. Sastry, A. Askell, P. Mishkin, J. Clark, et al. Learning transferable visual models from natural language supervision. In *International conference on machine learning*, pages 8748–8763. PMLR, 2021.

T. Ridnik, E. Ben-Baruch, A. Noy, and L. Zelnik-Manor. Imagenet-21k pretraining for the masses. *arXiv preprint arXiv:2104.10972*, 2021.

G. Ros, L. Sellart, J. Materzynska, D. Vazquez, and A. M. Lopez. The synthia dataset: A large collection of synthetic images for semantic segmentation of urban scenes. In *Proceedings of the IEEE conference on computer vision and pattern recognition*, pages 3234–3243, 2016.

C. Schuhmann, R. Vencu, R. Beaumont, R. Kaczmarczyk, C. Mullis, A. Katta, T. Coombes, J. Jitsev, and A. Komatsuzaki. Laion-400m: Open dataset of clip-filtered 400 million image-text pairs. *arXiv preprint arXiv:2111.02114*, 2021.

S. Sharifzadeh, S. M. Baharlou, and V. Tresp. Classification by attention: Scene graph classification with prior knowledge. In *Proceedings of the AAAI Conference on Artificial Intelligence*, volume 35, pages 5025–5033, 2021.

S. Sharifzadeh, S. M. Baharlou, M. Schmitt, H. Schütze, and V. Tresp. Improving scene

graph classification by exploiting knowledge from texts. In *Proceedings of the AAAI Conference on Artificial Intelligence*, volume 36, pages 2189–2197, 2022.

I. Shumailov, Z. Shumaylov, Y. Zhao, Y. Gal, N. Pernot, and R. Anderson. The curse of recursion: Training on generated data makes models forget. *arXiv preprint arXiv:2305.17493*, 2023.

G. Team, R. Anil, S. Borgeaud, Y. Wu, J.-B. Alayrac, J. Yu, R. Soricut, J. Schalkwyk, A. M. Dai, A. Hauth, et al. Gemini: a family of highly capable multimodal models. *arXiv preprint arXiv:2312.11805*, 2023.

N. Tritrong, P. Rewatbowornwong, and S. Suwanjanakorn. Repurposing gans for one-shot semantic part segmentation. In *Proceedings of the IEEE/CVF conference on computer vision and pattern recognition*, pages 4475–4485, 2021.

M. Tsimpoukelli, J. L. Menick, S. Cabi, S. Eslami, O. Vinyals, and F. Hill. Multimodal few-shot learning with frozen language models. *Advances in Neural Information Processing Systems*, 34:200–212, 2021.

G. Varol, J. Romero, X. Martin, N. Mahmood, M. J. Black, I. Laptev, and C. Schmid. Learning from synthetic humans. In *Proceedings of the IEEE conference on computer vision and pattern recognition*, pages 109–117, 2017.

R. Vedantam, C. Lawrence Zitnick, and D. Parikh. Cider: Consensus-based image description evaluation. In *Proceedings of the IEEE conference on computer vision and pattern recognition*, pages 4566–4575, 2015.

Z. Wang, J. Yu, A. W. Yu, Z. Dai, Y. Tsvetkov, and Y. Cao. Simvlm: Simple visual language model pretraining with weak supervision. *arXiv preprint arXiv:2108.10904*, 2021.

J. Zheng, J. Zhang, J. Li, R. Tang, S. Gao, and Z. Zhou. Structured3d: A large photo-realistic dataset for structured 3d modeling. In *Computer Vision–ECCV 2020: 16th European Conference, Glasgow, UK, August 23–28, 2020, Proceedings, Part IX 16*, pages 519–535. Springer, 2020.

J.-Y. Zhu, T. Park, P. Isola, and A. A. Efros. Unpaired image-to-image translation using cycle-consistent adversarial networks. In *Proceedings of the IEEE international conference on computer vision*, pages 2223–2232, 2017.

A. Appendix.

A.1. Extra Implementation details

A.1.1. VQ-GAN details

Table 6 | Configuration and training hyperparameters for VQGAN.

Config param	Value
Perceptual loss weight	0.05
Adversarial loss weight	0.01
Codebook size	8192
Optimizer	Adam (Kingma and Ba, 2014)
Discriminator learning rate	1e-4
Generator learning rate	1e-4
Optimizer momentum	$\beta_1=0.9 \beta_2=0.99$
Batch Size	256
Learning rate schedule	Cosine
Decay (Loshchilov and Hutter, 2017)	Warmup steps 10000
Training steps	500000

VQGAN Architecture: Our VQGAN architecture is similar to the previous work ([Esser et al., 2021](#)). It consists of several residual blocks, downsample (encoder) and upsample (decoder) blocks. The main difference is that we remove the non-local block to make the encoder and decoder fully convolutional to support different image sizes. In the base VQGAN model, we apply 2 residual blocks in each resolution and the base channel dimension is 128. For the finetuned decoder, we apply 4 residual blocks in each resolution and we also make the base channel dimension to be 256.

A.1.2. Optimization details for Synth²

Config param	Value
Optimizer	AdamW (Loshchilov and Hutter, 2017)
Learning rate	1e-4
Warmup steps	5e3
Weight Decay	1e-4
Gradient Clip	1.0

A.1.3. Text to image generator details

Config param	Value
Num Layers	12
Num Heads	12
Embedding hidden dim	768
MLP hidden dim	3072
Dropout	0.1
Codebook size	8192
Max Sample Length	64
Guidance Scale	4
Sample Temperature	32.5
Activation	GeLU

A.1.4. Perceiver details

Table 7 | Perceiver details

Config param	Value
Num Layers	6
Num Heads	16
Embedding hidden dim	1024
Activation	GeLU

A.2. Finetuning details

Following the pre-training stage, our model undergoes fine-tuning for various downstream tasks. The fine-tuning process employs the AdamW optimizer with similar Beta values as in pre-training. The learning rate was 1e-5.

To enhance generalization capabilities during fine-tuning, we utilize regularization methods such as Dropout (set to 0.1).

In accordance with established practices, we use the development split to determine optimal fine-tuning settings. The performance results are then reported based on the test split.

A.3. Clustering details

To determine the optimal number of clusters for our analysis, we employed the Elbow Method in conjunction with the Within-Cluster Sum of Squares (WCSS) metric. We iteratively applied the K-means clustering algorithm while varying the number of clusters, calculating the WCSS for each iteration. A clear ‘elbow’ point was observed in the WCSS plot, indicating a substantial decrease in variance as the number of clusters increased up to 20. Beyond this point, further increases in the number of clusters yielded diminishing returns in terms of WCSS reduction. Based on this analysis, we determined that 20 clusters provided a suitable balance between parsimony and capturing the underlying structure within our dataset.

To analyze the diversity of cluster compositions, we employed a co-clustering approach with the K-means algorithm on the concatenated GenPair, WebLI, and LTIP datasets. For each of the resulting

Table 8 | Zero shot image captioning results when using synthetically generated caption and image embedding pairs. Concentration is calculated as the cumulative distribution on the top-5 clusters, a lower value represent higher diversity (see Appendix A.3 for more details).

Real	Synth	#Real Data	#Synth Data	Concentration Top-3 (↓)	Concentration Top-5 (↓)	Entropy (↑)	CIDEr-COCO (↑)	Flickr-30(↑)	VQAV2 Acc. (↑)	OKVQA Acc. (↑)
CCv2	-	10.1M	-	-	-	-	22.1	12.7	29.1	32.4
CCv2	GenPair	10.1M	1M	40.5%	57.7%	3.81	25.9	17.3	31.1	34.0
CCv2+WebLI	-	10.1M+1M	-	58.2%	69.8%	3.43	24.4	14.9	30.6	33.9
CCv2+LTIP	-	10.1M+1M	-	76.5%	83.0%	2.92	23.4	13.8	30.3	32.9

Table 9 | Backbone ablation study. In this table the total amount of FLOPS (pre-training and training) was held constant

Model	real data	#params ↑	MSCOCO CIDEr ↑	VQAV2 Accuracy ↑
Synth ² VIT-B adapt.	690.1	632M	35.3	37.9
Synth ² VIT-L+ adapt.	690.1	890M	40.9	42.8
NFNet-F6 (CLIP)	690.1	920M	41.3	43.4

clusters, we calculated the normalized cluster sizes for each individual dataset. This allowed us to visualize the distribution among the datasets within each cluster, as illustrated in Figure 4.

To calculate the concentration we performed a cumulative sum over the top-5 clusters to determine what percentage of the data points was present there. The idea is that, the higher the percentage in the top 5 clusters, the less uniform is the distribution across all clusters, potentially indicating a lower level of diversity. Here in Table 8 we also report top-3 and the entropy over the full 20 clusters. Both measures confirm a more uniform distribution of data across clusters for GenPair versus the WebLI and LTIP. Especially the entropy complement the other measures as it takes into account all clusters, even if they are smaller.

A.4. Backbone Comparison

We conducted an ablation study to compare the performance of different visual backbones. For this comparison, we kept the total amount of FLOPs (both pre-training and training) and (self)supervised training data constant across models. We compared our VQ-GAN-based backbone against a contrastively pre-trained NFNet-F6 model (Brock et al., 2021) using the same loss function as CLIP (Radford et al., 2021). As shown in Table 9, the primary factor influencing performance appears to be the number of parameters, as our model with a deeper VQ-Adapter (VIT-L+) achieved results comparable to the contrastively trained model. In our study, we opted for the Synth²VIT-B backbone due to its compatibility with our hardware resources. This choice allowed us to avoid model sharding, thereby enabling faster experimental iterations.

A.5. Image Generator Qualitatives

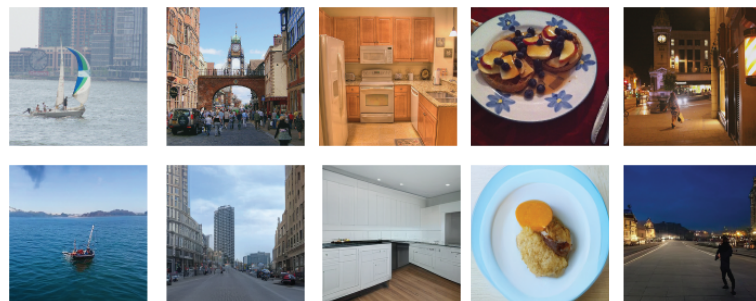


Figure 6 | Qualitatives showing images selected from the validation set of MS-COCO (Chen et al., 2015) (top row) and their synthetic versions generated by our text-to-image generator given the ground truth captions (bottom). The training of the image generator has been done on Conceptual Caption v2 (Changpinyo et al., 2021).